Electron Attachment and Detachment: Cyclooctatetraene

Thomas M. Miller* and A. A. Viggiano

Air Force Research Laboratory, Space Vehicles Directorate, 29 Randolph Road, Hanscom Air Force Base, Massachusetts 01731-3010

Amy E. Stevens Miller

ChemMotif, Inc., Suite 211, 60 Thoreau Street, Concord, Massachusetts 01742

Received: February 26, 2002; In Final Form: August 7, 2002

Electron attachment and detachment rate constants were measured for 1,3,5,7-cyclooctatetraene (COT) in a He/Ar buffer gas over the temperature range 295−365 K. A flowing afterglow Langmuir probe apparatus was used for this work. Within experimental uncertainty, the electron attachment rate coefficient is independent of temperature in this range, at a value of $3.5 \pm 1.0 \times 10^{-9}$ cm^3 s^{-1}. The electron detachment rate is negligible at room temperature, but climbs to 995 s^{-1} at 365 K. The attachment/detachment equilibrium constant implies that the electron affinity of COT is 0.57 ± 0.03 eV, in agreement with other studies using different methods. A vertical detachment transition from the planar anion leaves COT in a planar transition state for ring inversion. G2(MP2) and density functional calculations were carried out for COT neutral, anion, dianion, and the ring inversion transition state. The G2(MP2) ring inversion barrier height compares well with the experimental result from NMR studies.

Introduction

There is a large conformational change between 1,3,5,7-cyclooctatetraene neutral (COT; tub-like)[1,2] and anion (COT^-; planar),[3] to the point where there is no Franck−Condon overlap between the neutral and anion ground vibrational states.[4] Moreover, experiments by Wenthold et al.[4] have shown that photodetachment from the ground-state anion leaves the neutral in a planar transition state for ring inversion. Because of this, the photodetachment threshold energy is greater than the adiabatic electron affinity (EA) of COT by about 0.5 eV, and photodetachment cannot be used as a direct measure of the EA.

Measurements of EA(COT) have been made using the kinetic method (0.58 ± 0.04 eV),[5] by charge-transfer equilibrium (0.55 ± 0.02 eV),[6] and through electron/ion equilibrium using an electron capture detector (0.58 ± 0.04 eV).[7] The values are all in agreement with one another within the error limits placed on each. These values all indicated that we would be able to observe the thermal attachment and detachment of the electron in a flow tube at moderate temperatures. The question addressed in this paper is whether the unusual conformational change results in any peculiarity in thermal electron attachment and detachment processes, such as an unusual temperature dependence; the answer is that there is nothing atypical in the kinetics, although the attachment rate constant is rather small.

Experimental Section

A flowing-afterglow Langmuir-probe (FALP) apparatus was used in the present work.[8,9] In the FALP, a weak electron−He^+, $-Ar^+$ plasma was established in a fast flow of He/Ar buffer gas (133 Pa pressure, 1−2% Ar). Halfway down the 1-m long flow tube a known flow rate of COT vapor was added through a 3-needle inlet, and a movable Langmuir probe was used to measure the decay in the electron density as a function of distance along the flow tube axis, due to electron attachment. These data, coupled with measurements of the plasma velocity and diffusion coefficient, allow us to determine the electron attachment rate coefficient.[8,9] The only ion product of attachment observed was the parent anion (COT^-). EA(COT) is low enough that thermal electron detachment from COT^- occurs in the flow tube, so that extraction of rate constants from the raw data must include the electron detachment process.[10] Figure 1 shows a typical determination of the electron density as a function of distance down the flow tube, obtained at a temperature of 354 K and COT concentration of $n_r = 2.53 \times 10^{11}$ cm^{-3} (a partial concentration of about 10 ppmv). The measurements were taken over a flow tube distance of 35 cm with a plasma velocity of 10.2 m s^{-1}. The initial portion of the plot in Figure 1 is mostly governed by the magnitude of the electron attachment rate constant k_a. The later portion is influenced mostly by electron detachment from COT^-, with a rate constant k_d. Ambipolar diffusion is active over the entire reaction time. For determining the attachment and detachment rate constants, the optimum conditions[10] are that k_d and the attachment frequency ($= k_a n_r$) are similar in magnitude, and that k_d dominates over ambipolar diffusion (ν_D in Table 1). If $\nu_D > k_d$, the steady-state condition illustrated in Figure 1 is never reached.[10] For the data set shown in Figure 1 at 354 K these conditions are met; the attachment frequency ($= k_a n_r = 1030$ s^{-1} at the COT concentration given) is of the same order as the measured detachment rate ($k_d = 737$ s^{-1}), and both are larger than the diffusion frequency ($\nu_D = 398$ s^{-1}). We estimate uncertainties of ±35% for both the attachment and detachment rate constants.

COT was used as purchased,[11] except for several freeze−pump−thaw cycles. Mixtures of 1.8% COT in helium were made up for introduction into the flow tube through a helium-calibrated flowmeter.[12] COT was found to be "sticky" so that the glass mixture vessel required passivation, and the feedlines

* Corresponding author. E-mail: thomas.miller@hanscom.af.mil.

10.1021/jp0205214 CCC: $22.00
Published on Web 10/04/2002

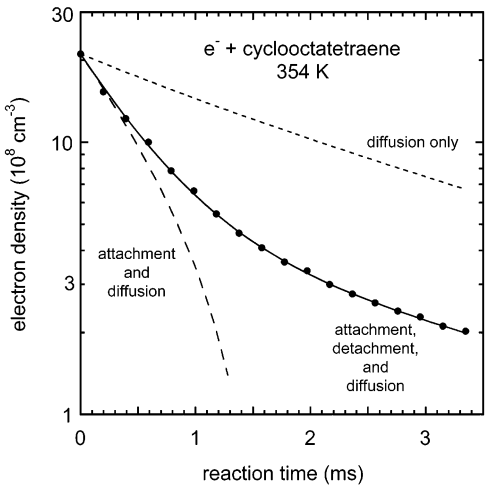

Figure 1. Electron density decay along the flow tube axis, showing the approach to a steady-state, diffusion-limited condition at long times. The solid line is a fit to the data of a solution to the rate equation governing free electron density loss due to attachment and diffusion, and electron density gain due to thermal detachment.

TABLE 1: Electron Attachment (k_a) and Detachment (k_d) Rate Constants for COT

T(K)	k_a (10^{-9} cm^3 s^{-1})[a]	k_d (s^{-1})[a]	ν_D (s^{-1})
295	3.3	(60)	291
317	3.2	(190)	329
329	3.2	300	317
339	4.1	493	371
354	3.9	739	398
365	3.3	995	454

[a] The experimental uncertainty is ±35% except that the k_d in parentheses are not reliable since they are smaller than the ambipolar diffusion rate, but give the best fit to the data. For comparison with k_d, the measured ambipolar diffusion decay constant ν_D is given for the electron−He^+, −Ar^+ plasma at 133 Pa pressure and ∼10 m s^{-1} plasma velocity.

needed as long as 45 min of passivation with the 1.8% COT mixture at room temperature. The low vapor pressure of COT and its stickiness led to greater uncertainty in the rate constants than usually experienced.

Results and Discussion

Table 1 gives the rate constants derived from the electron density data. Each reported rate constant is the average of 2−5 data sets at the same temperature. Within the reported experimental uncertainty, we do not observe any systematic variation in the electron attachment rate constant over the 295−365 K range; the average of the values determined over all temperatures is $3.5 \pm 1.0 \times 10^{-9}$ cm^3 s^{-1}. Comparison of this rate with that expected from the collisional rate constant given by Klots[13] shows that attachment occurs on about one of every 100 collisions at 295 K. The other collisions result in autodetachment before collisional or radiative stabilization of the electron−molecule complex can take place.

Recent experiments at Montana State University[14] using azulene as the attaching gas over a wide pressure range imply that higher buffer gas pressures are required to achieve complete thermal equilibrium in electron attachment/detachment experiments. It is not possible to test the pressure dependence appreciably using the FALP apparatus. The FALP buffer gas pressure may be varied from about 0.4 to 1.5 Torr, but ν_D is inconveniently large at low pressures. At higher pressures, gas flow around the reactant inlet needles causes a disturbance in the first half millisecond of reaction time, a region that is important for determining k_a. Furthermore, the Langmuir probe must be operated in a collisionless-sheath regime, a requirement which will be violated at high pressures, manifested by nonparabolic voltage−current characteristics.[9] Tests over the limited pressure range useful for us indicate that any error in k_d is covered by the ±35% uncertainty estimate. The largest single uncertainty is associated with n_r and is related to the very low vapor pressure of COT.

At each temperature the electron attachment and detachment rate constants were used to determine EA(COT) according to the procedure detailed in ref 10. The results quoted above for the data set at 354 K will be used as an example. The equilibrium constant was calculated ($K_a = k_a/k_d = 5.28 \times 10^{-12}$ cm^3) and the free energy for the attachment reaction determined ($\Delta G°_{354} = -0.566$ eV). The entropy change upon attachment can be estimated as due to the loss of the electron entropy on attachment, which is −0.254 meV mol^{-1} K^{-1} (yielding $T\Delta S° = -0.090$ eV at 354 K), and to the change in the entropy between COT and COT$^-$. The change in the entropy between COT and COT$^-$ is given by the sum of the electronic, rotational, and vibrational entropy changes (the change translational entropy, i.e., mass, is trivial). The electronic entropy change is just the ratio of spin degeneracies between COT (a singlet) and COT$^-$ (a doublet), since there are no other low-lying electronic states. The change in rotational entropy, to the extent that the rotational moments of inertia of ion and neutral are nearly equivalent, is given by the inverse ratio of rotational symmetry numbers for COT (D_{2d}, $\sigma = 4$) and COT$^-$ (D_{4h}, $\sigma = 8$). This is in the opposite ratio of the electronic entropy, and therefore the net change in the sum of the electronic and rotational entropy is zero. The vibrational entropy for COT and COT$^-$ will not fully cancel if there is an appreciable change in the vibrational frequencies upon electron attachment, but even for the dramatic conformational change, the vibrational frequencies do not change all that much on forming the anion. These qualitative predictions are confirmed by Møller-Plesset perturbation theory and density functional calculations described in the Appendix. The scaled Hartree−Fock results given in Table A1 yield a total entropy for COT$^-$ at 354 K of 3.648 meV mol^{-1} K^{-1}, and that for COT is 3.606 meV mol^{-1} K^{-1}, resulting in a net change of only +0.042 meV mol^{-1} K^{-1} and a contribution to the $T\Delta S°$ term of only +0.015 eV. For the overall electron attachment reaction, the $T\Delta S°$ term amounts to −0.075 eV, which is only a 13% adjustment to the free energy to obtain the enthalpy of attachment, $\Delta H°_{354} = -0.65$ eV.

The electron affinity is defined as the energy of attachment at 0 K, where the molecule, negative ion, and electron all have zero internal and translational energy. The enthalpy (energy) at 0 K is determined by adding 5 kT/2 for the electron thermal energy (0.076 eV at 354 K) to the enthalpy of the attachment reaction at temperature T, and then adding the difference in integrated heat capacities between COT and COT$^-$. The calculations described in the Appendix show that the integrated specific heats of COT and COT$^-$ almost cancel—the difference is only 0.004 eV at 354 K. The final result for the electron affinity is EA(COT) = 0.57 ± 0.03 eV, which is the average of the 4 data sets (such as shown in Figure 1) at 354−365 K for which optimum fitting conditions obtain, as was discussed earlier in this paper. The uncertainty in EA(COT) is based on assumption of worst-case 35% error in k_a and k_d, and a 5 K uncertainty in the gas temperature measurement and uniformity throughout the flow tube. We emphasize that the corrections for the difference in entropy and in the integrated

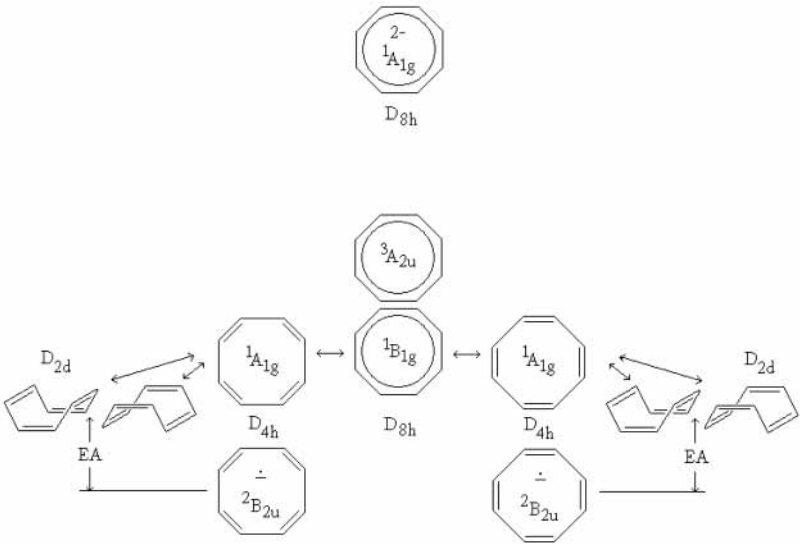

Figure 2. Neutral, anion, and dianion structures for COT. The vertical placement of a structure indicates its approximate relative energy.

heat capacity of COT and COT^- are quite small: the result is essentially independent of the calculated quantities given in the Appendix. Our value for the EA(COT) is in excellent agreement with the literature values,[5−7] that is, it falls within the range enclosed by the error limits of each determination. This agreement is a confirmation of the accuracy of our attachment and detachment rate constants from which our value for the EA is derived.

Note that $\Delta G°_T$ is determined solely from the equilibrium constant, which is in turn from the experimentally determined ratio of the attachment and detachment rate constants; the entropy corrections used to determine $\Delta H°_T$ are largely from the loss of the electron entropy. Since a *thermal* electron is attached/detached in this experiment, it is more useful to think of the "electron convention" in the thermochemistry.[15] The "ion convention" defines the electron temperature as if a zero-energy electron was formed (often a convenience in photoionization/photodetachment experiments where this is indeed the case),[15] and therefore the electron thermal energy contribution has to be added in explicitly in a thermal experiment such as this one. In any case, the EA, by definition, has a zero-energy electron and zero-energy ion, and is independent of the thermochemical convention used. Boltzmann statistics for the electron entropy and heat capacity were used for conversion of the enthalpy at temperature T to 0 K, consistent with standard usage of Chase et al. in the JANAF tables.[16] These authors pointed out that "at an electron partial pressure of 10^{-6} bar [7.5×10^{-4} Torr], the deviation between classical and quantum [Fermi-Dirac] statistics will be significant only below 5 K". At 354 K this pressure corresponds to an electron number density of 2.0×10^{13} cm^{-3}—well above the densities used for electron attachment in the FALP. Thermochemistry derived using Fermi-Dirac statistics for the electron has been presented,[16,17] but the traditional Boltzmann statistics were adopted in the JANAF compilations[16] and in recent reviews of gas-phase ion thermochemistry.[18,19]

Figure 2 shows a summary of the structures of the various states associated with COT and COT^-; it is based on experimental and theoretical results from refs 1−7, refs 20−23, and the present work.

Our value of EA(COT), 0.57 ± 0.03 eV, agrees quite well with previous work quoted in the Introduction. The photodetachment experiment of Wenthold et al.[4] measured the energy difference between the ground-state anion (D_{4h}, $^2B_{2u}$) and two planar neutral states, $^1A_{1g}$ and $^3A_{2u}$, of symmetries D_{4h} and D_{8h}, respectively. The $^1A_{1g}$ state is the transition state for ring inversion in COT, as indicated on Figure 2. Since EA(COT) is measured by other means, then the barrier height for ring inversion may be deduced from the $^1A_{1g} \leftarrow {}^2B_{2u}$ ion to neutral transition energy. Subtracting an average value of all experimental values (weighted by experimental uncertainties) of EA(COT), 0.57 eV, from the photodetachment transition energy (1.099 ± 0.010 eV)[4] yields the barrier to ring inversion in COT, 0.53 ± 0.04 eV (12.2 ± 1.0 kcal mol^{-1}). NMR work has provided an estimate of 0.43−0.48 eV for the activation energy for ring inversion in solution.[4,21−23] Multiconfiguration self-consistent field calculations for COT have been reported[20] and yielded a barrier height of 0.46 eV.

Though not particularly relevant to the present experiment, the dianion is shown in Figure 2; it is aromatic, in contrast to COT or COT^-, and is calculated (Appendix) to lie 2.67 eV above ground-state COT.

There are many examples in (nondissociative) electron attachment processes in which a large geometry change exists between neutral and anion. The most studied case is that of SF_6 (refs 8, 24, and references therein). Structural calculations for the neutral and anion[25] show elongation of S−F bonds upon electron attachment, but no change in the octahedral symmetry of the molecule. While the adiabatic electron affinity EA(SF_6) is relatively small (1.05 eV),[26] the vertical electron detachment energy for SF_6^- is quite large (3.16 eV)[27] because of the bond elongation. The rate constant for electron attachment to SF_6 is large, 2.3×10^{-7} cm^3 s^{-1} at room temperature,[8] and one may speculate on whether the conformational change has anything to do with this nearly collisional rate constant value. In this laboratory we have measured electron attachment rate constants for other single-center perfluoro compounds (SF_4,[8] PF_5,[28] MoF_6,[29] ReF_6,[29] and WF_6[29]) that form the parent anion upon attachment; the room-temperature rate constants range over 4 orders of magnitude, for reasons that are not understood. The SF_4 comparison with SF_6 is especially intriguing since the EAs are similarly moderate in magnitude and the vertical detachment energies are both large, although the SF_4 has both bond elongation and angle changes on forming the parent anion. SF_4 is far more chemically reactive than SF_6, yet SF_4 is found to attach thermal electrons at a rate 1/10th that of SF_6.[8]

The usual picture of electron attachment is that the electron is temporarily trapped in a resonant continuum state (the only way to explain the size of attachment cross sections), and

subsequently autodetaches, collisionally attaches, or radiatively attaches. In this picture, the different electron attachment rate constants are the result of the availability of resonant continuum states and the competition between autodetachment and stabilization. The structural difference between ground-state neutral and anion may not be as important as the presumably small structural difference between ground-state neutral and the continuum-state neutral to which the electron binds temporarily.

Conclusions

In the present work, we have measured the electron attachment rate constants for COT and detachment rate constants for COT^- over the temperature range 295−365 K. The attachment rate constant does not change significantly in this temperature range; the average value is $3.5 \pm 1.0 \times 10^{-9}$ cm^3 s^{-1}, which corresponds to an electron attachment efficiency of about 1%. The detachment rate constant is negligible at room temperature, but rises to 995 s^{-1} at 365 K. The equilibrium constant is used to determine the electron affinity of COT, 0.57 ± 0.03 eV, in agreement with earlier work. This result is also in agreement with that (0.52 eV) obtained from a G2(MP2) calculation detailed in the Appendix. The G2(MP2) result is expected to be good to better than 0.1 eV. Combining the experimental EA(COT) with the result of a photodetachment experiment[4] yields the height of the barrier to ring inversion in COT, 0.53 ± 0.04 eV. The G2(MP2) calculation gives 0.59 eV for this barrier height. The COT^{2-} dianion is calculated to lie 2.67 eV above ground-state COT.

Acknowledgment. We thank Prof. Paul Wenthold of Purdue University for discussions leading to this project and for critiquing the manuscript. We are grateful for continued support of this laboratory by the Air Force Office of Scientific Research. T.M.M. is under contract F19628-99-C-0069 to Visidyne, Inc., Burlington, MA.

Appendix

Calculations were carried out on COT and COT^- primarily to confirm the very small size of the entropy and heat capacity differences between anion and neutral, which enter into the conversion of the measured free energy of electron attachment to COT, into an electron affinity. At the same time, we were interested in how well the two theoretical methods used here could predict EA(COT), and where the dianion COT^{2-} lies in energy relative to COT. The GAUSSIAN-98W program package[30] was used in this work. The D_{2d} and D_{4h} symmetries of COT and COT^-, and the D_{8h} symmetry of COT^{2-}, were enforced in the calculations. Total energies were obtained using both second-order Møller−Plesset perturbation theory (MP2) and density functional theory (DFT). MP2 geometries were obtained using MP2(Full)/6-31G(d) as prescribed by the G2(MP2) formalism. DFT geometries were obtained using Becke's hybrid functional including the Lee−Yang−Parr correlation functional (B3LYP), with the Gaussian basis set denoted by 6-311+G(d,p). Frequency calculations verified that the structures were true minima and yielded zero-point energies. For the MP2 results, the frequency calculations were carried out with Hartree-Fock theory, using the 6-31G(d) basis set and scaling the frequencies by 0.8929.[31] For the DFT results, the frequency calculations were carried out using B3LYP/6-311+G(d,p), and scaled by 0.9613.[31,32] The transition state for ring inversion in COT has one imaginary frequency (negative force constant) corresponding to the inversion motion. The stability of each of the wave functions was checked, i.e., it was verified that the molecular orbital set chosen gave the lowest-energy wave function. To obtain EA(COT), total energies were improved using (a) the G2(MP2) method, which approximates a QCISD(T)/6-311+G(3df,2p) energy, and (b) B3LYP with the larger basis set 6-311+G(3df,2p) and tight convergence of SCF integrals. We have found the G2(MP2) method to be accurate to 0.1 eV for EAs, while the DFT result is not expected to be better than 0.3 eV. Table A1 gives the results of these calculations, focusing on data needed for the interpretation of the electron attachment experiment at 354 K. Molecular point groups and states are given in Figure 2. The G2(MP2) value for EA(COT), 0.52 eV, is in good agreement with experiment (0.55−0.58 eV), and well within the expected accuracy. The DFT EA(COT) is high, but not surprisingly so.

TABLE A1: Results of G2(MP2) and Density Functional Calculations (DFT) for the Lowest-Energy States of Neutral (D_{2d}) and Anionic (D_{4h}) COT (see Figure 2)

	G2(MP2)		DFT	
quantity	COT	COT^-	COT	COT^-
$S°_{354}$ (cal mol^{-1} K^{-1})[a]	83.2	84.1	84.0	85.5
$\int^{354} C_p\, dT$ (kcal mol^{-1})[a]	5.93	6.02	6.08	6.23
zero-point energy (h)[a]	0.12802	0.12412	0.12702	0.12434
total energy (0 K, h)[b]	−308.96503	−308.98431	−309.56370	−309.59743
EA (eV)[b]	0.52		0.91	
r(C−C) (Å)[c]	1.468	1.438	1.472	1.441
r(C=C) (Å)[c]	1.346	1.379	1.340	1.378
r(C−H) (Å)[c]	1.091	1.094	1.089	1.091

[a] HF/6-31G(d) level of theory (with frequencies scaled by 0.8929) for G2(MP2) results, and B3LYP/6-311+G(d,p) level of theory (with frequencies scaled by 0.9613) for DFT results. The entropy, $S°_{354}$, and the integrated specific heat, $\int^{354} C_p\, dT$, were evaluated at 354 K for interpretation of the electron attachment data. Hartree units are denoted by h. [b] G2(MP2) formalism, or B3LYP/6-311+G(3df,2p)//B3LYP/6-311+G(d,p) + ZPE for DFT results. [c] MP2(Full)/6-31G(d) for G2(MP2) results, and B3LYP/6-311+G(d,p) for DFT results.

TABLE A2: Ancillary Results for Two COT Transition States and the Dianion Ground State (see Figure 2)

	CASSCF	G2(MP2)	
quantity	COT bond switching transition state	COT ring inversion transition state	COT^{2-} dianion ground state
zero-point energy (h)[a]	−	0.12890	0.12037
total energy (0 K, h)[b]	−	−308.94318	−308.86693
r(CC) (Å)[c]	1.396	1.350, 1.470	1.416
r(CH) (Å)[c]	1.077	1.089	1.103

[a] HF/6-31G(d) level of theory, scaled by 0.8929. Hartree units are denoted by h. [b] G2(MP2) formalism. [c] CASSCF/6-31G(d) for CASSCF results, and MP2(Full)/6-31G(d) for G2(MP2) results.

Table A2 gives ancillary results for two COT transition states and the dianion ground state, for the specific states shown in Figure 2. Comparing the G2(MP2) total energy of the ring-inversion transition state with that of ground-state COT yields the barrier height for ring inversion, 0.59 eV (13.7 kcal mol^{-1}). This result is expected to be accurate within 0.1 eV and compares favorably with the 0.53 ± 0.04 eV (12.2 ± 1.0 kcal mol^{-1}) deduced from EA(COT) and the photodetachment transition energy to the ring-inversion transition state. The bond-switching transition state could not be studied with the G2(MP2) prescription as it requires a two-configuration method. Results using complete active space self-consistent field (CASSCF) methods were reported in ref 20, where the bond-switching barrier height was calculated to be 0.18 eV (4.1 kcal mol^{-1}).

The CASSCF energy is not given in Table A2 because it cannot be compared directly with the G2(MP2) or DFT energies given for the other molecules. The dianion is calculated to lie 2.67 eV above ground-state COT.

References and Notes

(1) Fray, G. I.; Saxton, R. G. *The Chemistry of Cyclooctatetraene and Its Derivatives*; Cambridge University Press: New York, 1978.

(2) (a) Paquette, L. A. *Tetrahedron* **1975**, *31*, 2855−2883. (b) Paquette, L. A. *Pure Appl. Chem.* **1982**, *54*, 987−1004. (c) Paquette, L. A. *Acc. Chem. Res.* **1993**, *26*, 57−62.

(3) Hammons, J. H.; Hrovat, D. A.; Borden, W. T.; Lineberger, W. C. *J. Am. Chem. Soc.* **1991**, *113*, 4500−4505.

(4) Wenthold, P. G.; Hrovat, D. A.; Borden, W. T.; Lineberger, W. C. *Science* **1996**, *272*, 1456−1459.

(5) Denault, J. W.; Chen, G.; Cooks, R. G. *J. Am. Soc. Mass Spectrom.* **1998**, *9*, 1141−1145.

(6) Kato, S.; Lee, H. S.; Gareyev, R.; Wenthold, P. G.; Lineberger, W. C.; DePuy, C. H.; Bierbaum, V. M. *J. Am. Chem. Soc.* **1997**, *119*, 7863−7864.

(7) Wentworth, W. E.; Ristau, W. J. *J. Phys. Chem.* **1969**, *73*, 2126−2133.

(8) Miller, T. M.; Miller, A. E. S.; Paulson, J. F.; Liu, X. *J. Chem. Phys.* **1994**, *100*, 8841−8848.

(9) Smith, D.; Španěl, P. *Adv. At. Mol. Phys.* **1994**, *32*, 307−343.

(10) Miller, T. M.; Morris, R. A.; Miller, A. E. S.; Viggiano, A. A.; Paulson, J. F. *Int. J. Mass Spectrom. Ion Processes* **1994**, *135*, 195−205.

(11) Aldrich Chemical, Milwaukee, WI.; purity 98%.

(12) MKS Instruments, Andover, MA. The COT/He mixture is so weak that the helium flow calibration is unaffected by the presence of COT.

(13) Klots, C. E. *Chem. Phys. Lett.* **1976**, *38*, 61−64. The polarizability of COT was estimated as 14 Å^3 based on results from the density functional calculations in the Appendix, and on the polarizabilities of similar-size hydrocarbon molecules given by Miller, T. M. In *Handbook of Chemistry and Physics*, 78th ed.; Lide, D. R., Ed.; CRC Press: Boca Raton, 1997; sect. 10, p 192.

(14) Williamson, D. H.; Knighton, W. B.; Grimsrud, E. P. *Int. J. Mass Spectrom.* **2000**, *195*/*196*, 481−489.

(15) Lias, S. G.; Bartmess, J. E.; Liebman, J. F.; Holmes, J. L.; Levin, R. D.; Mallard, W. G. Gas-Phase Ion and Neutral Thermochemistry. *J. Phys. Chem. Ref. Data* **1988** *17*, Suppl. 1, pp 8−10.

(16) Chase, M. W.; Davies, C. A.; Downey, J. R., Jr.; Frurip, D. J.; McDonald, R. A.; Syverud, A. N. *JANAF Thermochemical Tables*, third ed.; *J. Phys. Chem. Ref. Data* **1985**, *14*, Suppl. 1, p 1010.

(17) Bartmess, J. E. *J. Phys. Chem.* **1994**, *98*, 6420−6424. Bartmess, J. E. *J. Phys. Chem.* **1995**, *99*, 6755 (erratum).

(18) Rienstra-Kiracofe, J. C.; Tschumper, G. S.; Schaefer, H. F.; Nandi, S.; Ellison, G. B. *Chem. Rev.* **2002**, *102*, 231−282.

(19) Ervin, K. M. *Chem. Rev.* **2001**, *101*, 391−444.

(20) Hrovat, D. A.; Borden, W. T. *J. Am. Chem. Soc.* **1992**, *114*, 5879−5881.

(21) Anet, F. A. L. *J. Am. Chem. Soc.* **1962**, *84*, 671−672.

(22) Anet, F. A. L.; Boun, A. J. R.; Lin, Y. S. *J. Am. Chem. Soc.* **1964**, *86*, 3576−3577.

(23) Oth, J. F. M. *Pure Appl. Chem.* **1971**, *25*, 573−622.

(24) Španěl, P.; Matejcik, S.; Smith, D. *J. Phys. B: At. Mol. Opt. Phys.* **1995**, *28*, 2941−2957.

(25) Cheung, Y.-S.; Chen, Y.-J.; Ng, C. Y.; Chiu, S.-W.; Li, W.-K. *J. Am. Chem. Soc.* **1995**, *117*, 9725−9733. King, R. A.; Galbraith, J. M.; Schaefer, H. F. *J. Phys. Chem.* **1996**, *100*, 6061−6068.

(26) Grimsrud, E. P.; Chowdhury, S.; Kebarle, P. *J. Chem. Phys.* **1985**, *83*, 1059−1068.

(27) Datskos, P. G.; Carter, J. G.; Christophorou, L. G. *Chem. Phys. Lett.* **1995**, *239*, 38−43.

(28) Miller, T. M.; Friedman, J. F.; Miller, A. E. S.; Paulson, J. F. *Int. J. Mass Spectrom. Ion Processes* **1995**, *149*/*150*, 111−121.

(29) Miller, T. M.; Miller, A. E. S.; Viggiano, A. A. Unpublished work.

(30) Frisch, M. J.; et al. *GAUSSIAN 98W*, revision A.7; Gaussian, Inc.: Pittsburgh, PA, 1998.

(31) Foresman, J. B.; Frisch, Æ. *Exploring Chemistry with Electronic Structure Methods*, 2nd ed.; Gaussian: Pittsburgh, 1996; p 64.

(32) Miller, T. M.; Van Doren, J. M.; Morris, R. A.; Viggiano, A. A. *Int. J. Mass Spectrom.* **2001**, *205*, 271−276.